

Structural, Elastic and Thermal Properties of Lanthanide Monoantimonides

Muhammad Shafiq^{1,2*}, Imad Khan^{2,3}, Ijaz Ahmad^{2,3}, Zahid Ali^{2,3}, S Jalali-Asadabadi⁴, Iftikhar Ahmad^{1,2} Amel Laref⁵ and Yasir Saeed¹¹Department of Physics, Abbottabad University of Science & Technology, Havelian, Pakistan²Center for Computational Materials Science, University of Malakand, Pakistan³Department of Physics, University of Malakand, Chakdara, Pakistan⁴Department of Physics, Faculty of Sciences, University of Isfahan, HezarGerib Avenue, Isfahan 81744-73441, Iran⁵Department of Physics and Astronomy, College of Science, King Saud University, Riyadh, 11451 King Saudi Arabia

*Corresponding author

Muhammad Shafiq, Department of Physics, Abbottabad University of Science & Technology, Havelian, Pakistan, E-Mail: shafiqdurranium@gmail.com

Submitted: 28 Jan 2018; Accepted: 15 Feb 2018; Published: 16 Apr 2018

Abstract

Structural, elastic and thermal properties of lanthanide monoantimonides LnSb ($\text{Ln} = \text{La}, \text{Ce}, \text{Pr}, \text{Nd}, \text{Sm}, \text{Gd}, \text{Tb}, \text{Dy}, \text{Ho}, \text{Er}, \text{Tm}, \text{Yb}$ and Lu) compounds have been studied theoretically using full potential linearized augmented plane wave plus local orbitals (FP-LAPW + lo) method within the density functional theory. The structural properties are investigated by using GGA-PBESol scheme. We calculated bulk modulus, shear modulus, Young's modulus, anisotropic ratio, Kleinman parameters, Poisson's ratio, Lamé's co-efficient, sound velocities for shear and longitudinal waves, and Debye temperature. We also predict the Cauchy pressure and B/G ratio in order to explore the ductile and brittle behaviors of these compounds. Our results are in good agreement with available experimental and other theoretical data and also provide predictions where no experimental or theoretical results are available.

Keywords: Monoantimonides, Cubic-Elastic Software, Elastic Constants, Mechanical Properties

Introduction

Lanthanide-based monpnictides LnX ($\text{Ln} = \text{La}, \text{Ce}, \text{Pr}, \text{Nd}, \text{Sm}, \text{Gd}, \text{Tb}, \text{Dy}, \text{Ho}, \text{Er}, \text{Tm}, \text{Yb}$ and Lu and $\text{X} = \text{P}, \text{As}, \text{Sb}$ and Bi) attract great attention due to their interesting electronic and magnetic properties and a variety of practical applications in the field of non-linear optics, glass making, phosphors lasers, composites lasers, displays, metal based transistor and optical amplifiers. These compounds are simple cubic NaCl type crystal also exhibit many unusual physical properties such as large magnetic anisotropy, complex magnetic phase diagram, large Kerr angle, heavy-fermion, mixed-valence, Kondo insulator and very small crystal field splitting [1-4]. These phenomena are intimately connected with the strong correlations among the Ln-f and pnictide-p electrons and the proper theoretical description of the electronic structures of these compounds remains a challenge [4,5]. The electronic properties of the lanthanides based compounds are solely dependent on the degree of localization and itinerant nature of f electrons. The rare-earth elements exhibit different degrees of localization. The light lanthanides like Ce, Pr and Nd are weakly delocalized whereas the heavier lanthanides rare-earths are strongly localized [3]. Further, the bonding between the Ln and pnictogen atoms cannot simply be described as ionic or covalent, otherwise they would all be expected to be insulators (semiconductors) [6].

Among the lanthanide pnictides, the lanthanide antimonides (LnSb) have recently attracted particular interest as a proper reference material for understanding of various elastic, structural and magnetic effects [7]. Some of them show magnetic and crystallographic phase transitions at low temperatures. Monoantimonides (CeSb, SmSb and YbSb) with NaCl-type structure exhibit anomalies in various physical properties due to the p-f mixing, dense Kondo effect and heavy fermion state. Their carrier concentrations increase with decreasing temperature since the p-f mixing becomes stronger. On the other hand, other rare-earth monoantimonides behave as a nearly normal magnetic semi-metals and display almost temperature-independent carrier concentrations [7].

So far as the structural properties are concerned, several pnictides of lanthanide group are crystallized in NaCl (B1) type crystal structure and have been investigated by using high-pressure X-ray diffraction technique and reported to undergo either CsCl (B2) or body centered tetragonal (BCT) structure [8-10]. Various experimental studies have been done to investigate the electronic properties of these compounds [11-13]. The elastic constants of LaSb and Gd monpnictides were reported experimentally [14,15]. Rakshit, et al. investigated the lattice vibrational properties of $\text{LaSb}, \text{CeSb}, \text{PrSb}$ and NdSb using Raman scattering technique (RST) [13]. The optical properties of SmSb and TmSb are studied by Gigineishvili, et al. [16]. The magnetic properties of $\text{NdSb}, \text{GdSb}, \text{TbSb}, \text{DySb},$

HoSb and ErSb have been studied by Missell, et al. [17].

Besides experiments, lanthanide monoantimonides are also extensively studied theoretically. Bhajanker, et al. investigated the thermal and mechanical properties of praseodymium monopnictides by two body interionic potential (TBIP) [18]. Electronic, structural, phonon, elastic and thermodynamical properties of SmX (X = P, Sb and Bi) TmSb and GdSb compounds are calculated using pseudo potential GGA approximation [19-21]. Svane, et al. studied the lattice parameters and bulk modulus of Samarium pnictides by means of self-interaction corrected local spin density approximation (SIC-LSDA) [22]. The structural, elastic and thermal properties of Ho, Er and Tm antimonides have been calculated by Soni, et al. by simple interionic potential. Pagare, et al. using two body interionic potential to investigate theoretically high pressure structural phase transition and cohesive properties of DySb and LuSb [23,24].

Though lanthanide monoantimonides are extensively studied both experimentally and theoretically but there is a lack of comprehensive theoretical study of this series of compounds. In the present work we report the structural and elastic properties of these versatile compounds using generalized gradient approximation (GGA-PBEsol). Attempt has been made to get rational theoretical foundations to the experimental measurements and provide detailed information of several unexplored mechanical and thermal properties.

Computational details

Calculations are performed using full-potential linearized augmented plane waves plus local orbital (FP-LAPW + lo) [25] method as implemented in the WIEN2k package [25,26]. For structural properties spin-polarized calculations are carried out using generalized gradient approximation (GGA-PBEsol) [27] as an exchange-correlation potential. In full potential scheme, the wave functions inside the non-overlapping spheres are expanded as spherical harmonics up to angular momentum $l = 10$. Plane wave expansion is used in the remaining space of the unit cell (interstitial region) fixing the parameter $R_{MT} K_{max} = 7$. RMTs are chosen in such a way that no charge leakage occurred from the core and total energy convergence is ensured. We have used 3000 k-points in the Brillouin zone (BZ) integration. The self-consistent calculations were considered to converge only when the calculated total energy of the crystal converges to less than 10^{-4} Ry. The total energies were further used to obtain the ground state properties.

Elastic constants are the key parameters for the determination of the mechanical properties of a material. In the present work the elastic constants of LnSb (Ln = La, Ce, Pr, Nd, Sm, Gd, Tb, Dy, Ho, Er, Tm, Yb and Lu) compounds are calculated using Cubic-elastic software implemented in WIEN2k code [28]. The details about Cubic-elastic software are available in Refs. [28,29]. In particular a cubic lattice has only three independent elastic constants C_{11} , C_{12} and C_{44} .

These constants are calculated, and are further used to evaluate the mechanical properties of LnSb compounds such as the shear modulus (G_H), Young's modulus (Y), Cauchy pressure (C''), Poisson's ratio (ν), Kleinman parameter (ζ), and anisotropy constant (A) using standard relations.

Results and Discussions

Structural properties

The spin polarized calculations are carried out using GGA flavor GGA-PBEsol for structural properties of LnSb (Ln = La, Ce, Pr, Nd, Sm, Gd, Tb, Dy, Ho, Er, Tm, Yb and Lu) in NaCl crystal structure. The structural parameters like lattice constant and bulk modulus are obtained by minimizing the total energy versus volume for LnSb compounds. The Birch-Murnaghan's Fit equation of states is used for optimization [30]. The calculated parameters of these compounds are compared with available experimental and theoretical results and listed in Table 1. The table shows that our calculated results of the lattice constants are in agreement with experimental measured values. The calculated results of the lattice constant are also compared with the experimental values in Fig. 1. The figure indicates that lattice constant of LnSb compound shrinks with increasing the number of f electrons which can be attributed to the lanthanide contraction along the lanthanide series from La to Lu. This trend in lattice constant can be explained by increased anion size and decreased cation size with increased atomic number [31].

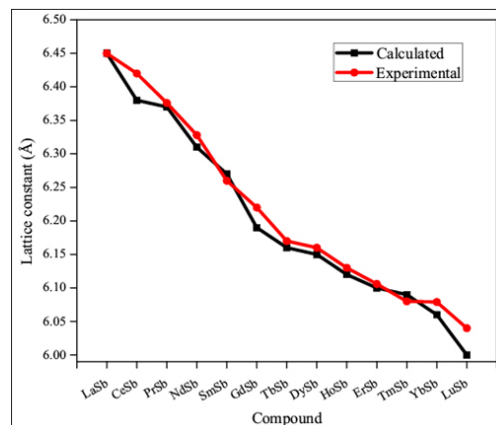


Figure 1: Comparison of Calculated and experimental lattice constants.

The bulk modulus B_0 is another important parameter and is a measure of resistance to volume change by applied pressure or the resistance to fracture. High value of B_0 has greater resistance to fracture. The calculated values of B_0 are presented in Table 1. It is evident from the table that our calculated values of bulk modulus are in close agreement with reported experimental and other theoretical results. LaSb has a high value of B_0 is 74.67 GPa among rare-earth antimonides confirming greater resistance to fracture, while PrSb has a small value of 48.56 GPa in this series.

Table 1: Calculated lattice constant (\AA) and bulk modulus (GPa) of LnSb compounds in B1 structure

Compounds		E_{xc}	A	B_o
LaSb	Theory Experiment	Present GGA ^{PBE-sol}	6.45	74.67
		LDA ^d	6.30	69.76
		WC-GGA ^c	6.46	59.20
			6.49 ^b , 6.45 ^c	71.5±3
CeSb	Theory Experiment ^b	Present GGA ^{PBE-sol}	6.38	72.3
		SIC-LSDf	6.36	69.2
			6.42	71.5
PrSb	Theory Experiment	Present GGA ^{PBE-sol}	6.37	48.56
		SIC-LDA ^g	6.24	55
		IPT ^h	6.40	53.5
			6.376 ^a , 6.384 ⁱ	44±5 ^j
NdSb	Theory Experiment ⁱ	Present GGA ^{PBE-sol}	6.31	55
			6.328	58.70
SmSb	Theory Experiment ^a	Present GGA ^{PBE-sol}	6.27	66.76
		GGA ^k	6.32	56.90
		SIC-LDA ^l	6.30	46.7
			6.26	-----
GdSb	Theory Experiment	Present GGA ^{PBE-sol}	6.19	62.78
		GGA ^m	6.25	58.74
		LSDA ⁿ	6.13	65.29
		LSDA+U ^o	6.39	-----
			6.22 ^{a,p}	63.71 ^p
TbSb	Theory Experiment ^a	Present GGA ^{PBE-sol}	6.16	71.93
			6.17	
DySb	Theory Experiment ^a	Present GGA ^{PBE-sol}	6.15	55.80
		MIPM ^q	6.16	53.42
HoSb	Theory Experiment ^a		6.12	63.37
			6.13	
ErSb	Theory Experiment ^a	Present GGA ^{PBE-sol}	6.10	69.68
		LDA ^r	6.08	68.18
			6.106	70.93
TmSb	Theory Experiment	Present GGA ^{PBE-sol}	6.09	71.27
		GGA-PBE ^s	6.1	60.71
		LSDA+U ^t	6.06	57.41
		LDA ^r	6.03	71.04
			6.105 ^u , 6.08 ^v	71.73 ^a
YbSb	Theory Experiment	Present GGA ^{PBE-sol}	6.06	57.23
		LSDA+U ^t		59.30
			6.079 ^a	52±2 ^w
LuSb	Theory Experiment ⁱ	Present GGA ^{PBE-sol}	6.00	57.8
		GGA+U ^x	6.09	60.69
		GGA ^y	6.11	58.04
			6.04	53±4

^a [12], ^b[9], ^c[32], ^d[33], ^e[34], ^f[4] ^g[35], ^h[36], ⁱ[37], ^j[38], ^k[19], ^l[22], ^m[21], ⁿ[39], ^o[40], ^p[15], ^q[7], ^r[41], ^s[20], ^t[42], ^u[43], ^v[44], ^w[45], ^x[6], ^y[24]

Elastic and mechanical properties

The elastic constants provide important information about the binding characteristics between the closest atomic planes, stiffness stability and anisotropic character of binding of the materials. They also provide a relationship between the dynamical and mechanical behaviors of materials and give important information related to the nature of forces acting in solids [46,47]. The elastic stiffness constant C_{11} represents elasticity in length, and C_{12} and C_{44} are shape related elastic constants. The calculated second order elastic constants (SOECs) C_{11} , C_{12} and C_{44} for LnSb (Ln = La, Ce, Pr, Nd, Sm, Gd, Tb, Dy, Ho, Er, Tm, Yb and Lu) compounds, with available experimental and other theoretical results are listed in

Table 2. It is clear from the table that our calculated results satisfy the conditions for mechanical stability, i.e., $C_{11} + 2C_{12} > 0$, $C_{11} - C_{12} > 0$, $C_{11} > 0$, $C_{44} > 0$ and $C_{12} < B < C_{11}$ for cubic structures, hence these compounds are stable against elastic deformation [48,49]. Our calculated values of C_{44} for the compounds under investigation are in excellent agreement consistent with experimental results, as compared to other theoretical reported results presented in Table 2. The calculated difference between two elastic constants C_{11} and C_{12} , i.e., $C_{11} - C_{12}$ for LnSb compounds show slightly disagreement as compared to the available experimental measured value, but our results are better for these compounds as compared to the other theoretical results.

Table 2: Calculated second order elastic constants (SOECs) in GPa of LnSb compounds in B1 structure

Comp.		C_{11}	C_{12}	C_{44}	$C_{11}-C_{12}$
LaSb	Present	94.77	12.72	19.96	82.05
	Theory	159.5 ^b , 132 ^c , 140 ^d	19.9 ^b , 15 ^c , 20 ^d	5.0 ^b , 19.7 ^c , 21 ^d	139.6 ^b , 117 ^c , 120 ^d
	Exp. ^a			19.5	74.0
CeSb	Present	108.53	14.81	18.34	93.72
	Theory ^e	146.42	24.44	24.44	
PrSb	Present	118.99	13.82	21.13	105.02
	Theory	117 ^f , 117.01 ^g	21 ^f , 21.75 ^g	21 ^f , 21.80 ^g	96.0 ^f
	Exp. ^a			20.0	110.0
NdSb	Present	124.73	16.30	17.37	117.02
	Theory ^e	110.56	22.35	22.35	
SmSb	Present	132.83	19.62	19.89	125.2
	Theory ^h	82.11	4 4.29	5.61	37.82
	Exp. ^a			22.7	127
GdSb	Present	135.2	12.55	24.04	122.61
	Theory	123.38 ⁱ , 40.01 ^j , 83.64 ^k	29.34 ⁱ , 8.41 ^j , 6.29 ^k	29.34 ⁱ , 8.61 ^j , 5.96 ^k	94.04 ⁱ , 31.6 ^j , 37.35 ^k
TbSb	Present	142.20	15.89	21.12	126.31
DySb	Present	157.738	17.435	30.194	140.348
	Theory ^l			22.36	100.87
	Exp. ^a			26.00	148.00
HoSb	Present	148.87	14.72	25.78	134.15
	Exp. ^a			27.6	138.00
ErSb	Present	112.69	15.89	24.68	128.58
	Theory ^l	113.65	16.98	19.57	96.67
	Exp. ^a			26.0	135
TmSb	Present	151.55	19.02	27.06	132.53
	Theory	151.898 ^m , 160.9 ⁿ	17.289 ^m , 24.5 ⁿ	25.42 ^m , 24.7 ⁿ	134.609 ^m , 136.4 ⁿ
	Exp. ^a			26.8	135
YbSb	Present	134.33	18.71	24.62	115.62
LuSb	Present	128.57	21.80	25.61	106.77
	Theory	122.77 ^o , 147.64 ^o	23.14 ^o , 18.63 ^o	23.34 ^o , 25.96 ^o	99.63 ^o

^a[12], ^b[50], ^c[51], ^d[14], ^e[8], ^f[18], ^g[36], ^h[19], ⁱ[15], ^j[52], ^k[21], ^l[24], ^m[20], ⁿ[23], ^o[6]

The elastic constants determine the response of the crystal to external forces, as characterized by Young's modulus, shear modulus, anisotropic ratio, and Poisson's ratio, and play an important role in determining the strength, stability, internal strain, thermo elastic stress, sound velocity, fracture, toughness of materials. The mechanical parameters such as shear modulus (G_H), Young's modulus (Y), B/G ratio, Cauchy pressure (C''), Poisson's ratio (ν), Kleinman's parameter (ζ), anisotropy factor (A) and shear constant (C') are listed in Table 3.

The shear modulus $G = G_H$ describes the material's response to shearing strain and to obtain G we used Voigt shear modulus G_V and Reuss shear modulus G_R using the relations [52-55]:

$$G_V = \frac{1}{5}(3C_4 + C_1 - C_2) \quad (1)$$

$$G_R = \frac{5(C_1 - C_2)C_4}{4C_4 + 3(C_1 - C_2)} \quad (2)$$

Shear modulus is the arithmetic means of G_V and G_R :

$$G = \frac{G_V + G_R}{2} \quad (3)$$

The greater value of shear modulus for DySb (42.64GPa) confirm that this compound show more resistance to plastic deformation while LaSb has less resistance to plastic deformation. The smaller values of shear modulus for all these compounds reveal that, these all material offer less resistance to plastic deformation.

The Young's modulus gives useful information about the stiffness of materials and can be calculated using the following equation:

$$Y = \frac{9BG_V}{3B + G_V} \quad (4)$$

Larger the value of Y , the stiffer is the material. It is clear from Table 3 that DySb is stiffer in all these LnSb compounds.

Pugh proposed the brittle/ductile nature of compounds by the ratio of bulk modulus to shear modulus (B/G) [56]. If B/G ratio is less than 1.75, the material behaves in a brittle manner, otherwise the material will be ductile. It is evident from Table 3 that all compounds show brittle nature ($B/G < 1.75$). The Cauchy's pressure, which is the difference between C_{12} and C_{44} ($C' = C_{12} - C_{44}$) can be also used to describe the brittle/ductile nature of materials. Pettifor suggested that the corresponding negative/positive value of Cauchy's pressure is responsible for the brittle/ductile nature of a compound [57]. The calculated value of Cauchy's pressure for LnSb compounds presented in Table 3 indicates that all these compounds show brittle behavior. The Cauchy's pressure is also used to predict the bonding character in a material. Its positive value indicates the ionic bonding while the negative Cauchy's pressure attribute to directional bonding (covalent bonding). It is clear from Table 3 that all these compounds have negative Cauchy's pressure, and hence these compounds possess directional (covalent) bonding nature.

Another parameter which also described the brittle/ductile nature of a compound is Poisson's ratio which can be calculated using the relation:

$$\nu = \frac{3B - Y}{6B} = \frac{1}{2} - \frac{Y}{6B} \quad (5)$$

The Poisson's ratio lies in between -1.0 and 0.5 , which are the lower and upper bounds. The lower bound is where the materials do not change its shape and the upper bound is where the volume remains unchanged. On the basis of Poisson's ratio Frantsevich, et al. explained the brittle/ductile nature of compounds; the compounds are brittle if ν less than 0.33 , otherwise the compounds are ductile [32]. The calculated values of ν for LnSb compounds for all compounds under study is less than 0.33 , hence the brittle nature for LnSb are further confirm in term of Poisson's ratio. If $\nu \rightarrow 0$ the materials are more compressible [58]. Our calculated values of Poisson's ratio are greater than zero ($\zeta=1 \rightarrow 0.2$), show that these materials are less compressible and stable against deforming force.

Kleinman's parameter (ζ), describes the relative positions of the cation and anion sublattices under volume conserving strain distortions for which positions are not fixed by symmetry [21]. A low value of $\zeta=0$ implies a large resistance against bond bending or bond-angle distortion and upper limit $\zeta=1$ leads to bond stretching. [59-61]. The Kleinman's parameter can be calculated from elastic constants by using the following relation:

$$\zeta = \frac{C_1 + 8C_2}{7C_1 - 2C_2} \quad (6)$$

The calculated values in Table 3 predicted the bond stretching is dominant in LnSb compounds (lower limit of ζ).

The elastic anisotropic factor A gives a measure of the anisotropy of the materials and closely related to the microcracks in a material. Anisotropic ratio can be calculated by using the following equation:

$$A = \frac{2C_4}{C_1 - C_2} \quad (7)$$

For isotropic material, A is unity. From Table 3, we can see that the calculated anisotropic ratio of LnSb compounds deviate from unity, means that these compound show anisotropic character and their properties vary in different directions.

Another mechanical parameters are Lamé's constants (λ, μ), which measure hardness of the materials. Using Young modulus and Poisson's ratio, Lamé's constants λ and μ can be obtain by the following equations:

$$\lambda = \frac{Y\nu}{(1+\nu)(1-2\nu)} \quad (8)$$

$$\mu = \frac{Y}{2(1+\nu)} \quad (9)$$

The first Lamé's constant (λ) is a measure of the compressibility of a material, the second Lamé's constant (μ), reflects shear stiffness [62]. The values of Lamé's constants for LnSb compound are given in Table 3. From the Table 3, it is clear that our calculated value of Lamé's second modulus is equal to Voigt's shear modulus (i.e., $\mu = G_V$). For isotropic materials $\lambda = \mu = C'$ and $\mu = C'$. As LnSb compounds are strongly anisotropic, hence does not satisfied the condition of isotropy, i.e., $\lambda = C_{12}$ and $\mu = C'$.

Shear constant (C'), also known as tetragonal shear modulus, it is one of the criterions of mechanical stability and shows the stability of the tetragonal distortion. For dynamical stability the shear constant >0 and has been calculated by using the following relation:

$$C' = \frac{C_{11} - C_{12}}{2} \quad (10)$$

It is clear from Table 3 that our calculated value for C' is positive for all compounds which indicate that these compounds are mechanically stable.

Table 3: The calculated value of Voigt's shear modulus G_V , Reuss's shear modulus G_R , Hill's shear modulus G_H , B/G ratio, Cauchy Pressure (C''), Poisson's ratio (ν), Kleinman Parameter (ζ), Anisotropy constant (A) Lames Coefficient (λ and μ), and Shear Constant (C').

Table 3: The calculated value of Voigt's shear modulus G_V , Reuss's shear modulus G_R , Hill's shear modulus G_H , B/G ratio, Cauchy Pressure (C''), Poisson's ratio (ν), Kleinman Parameter (ζ), Anisotropy constant (A) Lames Coefficient (λ and μ), and Shear Constant (C').

Comp	LaSb	CeSb	PrSb	NdSb	SmSb	GdSb	TbSb	DySb	HoSb	ErSb	TmSb	YbSb	LuSb
G_V	28.39	29.75	33.71	34.51	36.38	38.95	37.93	46.18	42.30	34.17	42.74	37.90	36.72
G_R	25.12	24.24	27.78	28.20	30.05	31.77	28.78	39.10	34.20	30.70	35.45	31.96	32.34
G_H	26.75	26.99	30.74	31.36	33.21	35.36	33.36	42.64	38.25	32.43	39.10	34.93	34.53
Y	68.89	73.43	82.23	84.90	90.08	94.02	93.43	111.74	102.56	82.90	104.64	93.14	90.80
B/G	1.50	1.71	1.59	1.67	1.73	1.51	1.74	1.51	1.55	1.48	1.62	1.64	1.66
C''	-7.24	-3.53	-7.31	-5.07	-3.27	-11.49	-5.23	-12.76	-11.06	-8.79	-8.04	-5.91	-3.81
ν	0.21	0.23	0.22	0.23	0.24	0.21	0.23	0.21	0.21	0.21	0.22	0.23	0.24
ζ	0.31	0.31	0.29	0.30	0.33	0.26	0.28	0.28	0.26	0.32	0.30	0.31	0.35
A	0.49	0.39	0.40	0.39	0.40	0.39	0.33	0.43	0.38	0.51	0.41	0.43	0.48
λ	21.15	26.22	26.40	32.94	35.78	27.46	32.70	33.42	31.24	25.38	34.70	31.99	32.91
μ	28.39	29.75	33.71	34.08	36.06	38.95	37.93	46.18	42.30	34.17	42.74	37.90	36.72
C'	41.03	46.86	52.59	54.22	56.61	61.33	63.16	70.16	67.08	48.40	66.27	57.81	53.39

Thermal Properties

Debye temperature (θ_D) is that temperature at which the wave length λ of vibrating atom is equal to the length of the unit cell in a crystal. It is important parameter which closely related to elastic constants, melting temperature and specific heat. We calculated Debye temperature by using the relation [63, 64].

$$\theta_D = \frac{h}{k_B} \left[\frac{3n}{4\pi} \left(\frac{\rho N_A}{M} \right) \right]^{\frac{1}{3}} v_m \quad (11)$$

Where K_B is Boltzmann's constant, h is plank constant, ρ is density of a compound, n is number of atom in a unit cell, N_A is Avogadro number, M is the molecular mass of a compound and v_m is average speed of sound, which is calculated as [65]:

$$v_m = \left[\frac{1}{3} \left(\frac{2}{v_t^3} + \frac{1}{v_l^3} \right) \right]^{-\frac{1}{3}} \quad (12)$$

Where v_t and v_l are the transverse and longitudinal waves velocities respectively which is obtained from the equations [66]:

$$v_t = \left[\frac{G}{\rho} \right]^{\frac{1}{2}} \quad (13)$$

It is clear from above equations that the sounds velocities are directly related to the shear modulus G and bulk modulus B . greater the value of G and B greater will be the value of sounds velocities.

Our calculated value of density, longitudinal v_l , transverse v_t , average sound velocities v_m and the Debye temperature for LnSb (Ln = La, Ce, Pr, Nd, Sm, Gd, Tb, Dy, Ho, Er, Tm, Yb and Lu) compounds are listed in Table 4. We compared our calculated results to available experimental as well as others theoretical results. Our calculated values for Debye temperature (θ_D) are overestimated than the available experimental results, but are comparable to the experimental results than other theoretical reported results. Our calculated value for Debye temperature θ_D for these compounds at 0K is higher than experimental data of Mullen et al., ($T = 200$ K) listed in table 4, due to fact that at constant pressure the Debye temperature decreases as temperature increases [21]. For high value of θ_D the compound will be stiffer and exhibit high thermal conductivity. It is clear from the Table 4 that θ_D for DySb ($\theta_D = 309.71$ K) is stiffer than the other compound in LnSb series due to higher value of Young modulus and elastic constants.

Table 4: The calculated values of density ρ (g/cm³), sound velocity of transverse wave v_t (m/s), sound velocity of longitudinal waves v_l (m/s), average velocity v_m (m/s) and Debye temperature θ_D (K) of compounds.

Comp.		ρ	v_t	v_l	v_m	θ_D
LaSb	Present	6.45	3426.20	2036.26	2254.66	262.25
	Exp. ^a	6.33				211.00
CeSb	Present	6.70	3499.51	2007.36	2229.81	262.27
	Exp. ^a	6.77				221.00
	Other ^b	6.66	3804.00	2197.00	2439.00	360.00
NdSb	Present	7.03	3660.92	2111.59	2344.46	278.75
SmSb	Present	7.33	3722.62	2127.98	2364.50	282.92
	Exp. ^a	7.37				232.00
	Other ^c		3113.30	1143.90	1298.80	77.100
GdSb	Present	7.82	3587.46	2127.09	2355.76	285.63
	Exp. ^a	7.70				233.00
	Other ^{d,e}		4086.19, 2980.9	2274.51	2532.85	157.2, 148.88, 246.45 ^d
TbSb	Present	7.98	3584.27	2045.05	2272.71	276.88
DySb	Present	8.12	3861.95	2292.03	2538.20	309.71
HoSb	Present	8.31	3646.16	2145.83	2378.17	291.60
ErSb	Present	8.46	3287.09	1958.08	2167.09	266.59
	Exp. ^a	8.42				237.00
	Other ^f					252.00
TmSb	Present	8.55	3672.68	2138.39	2372.24	292.29
	Exp. ^a	8.57				237.00
	Others ^g	8.70	3645.50	2216.20	2448.50	241.00
YbSb	Present	8.80	3434.88	1992.30	2210.88	273.75
	Other ^e	8.80	3580.00	2096.00	2324.10	228.00
LuSb	Present	9.12	3367.08	1945.49	2159.72	270.04
	Other ^h		3658.90	2177.74	2410.98	235.70
	Other ⁱ		3419.00	1929.00	2144.00	205.00

^a[12], ^b[18], ^c[19], ^d[21], ^e[39], ^f[7], ^g[42], ^h[6], ⁱ[24]

Conclusion

First principle calculations have been performed to investigate structural, elastic, mechanical and thermal properties of LnSb (Ln = La, Ce, Pr, Nd, Sm, Gd, Tb, Dy, Ho, Er, Tm, Yb and Lu) compounds using (FP-LAPW + lo) method within density functional theory. The ground state lattice parameters are consistent with experiment and exhibit lanthanide contraction. Mechanical properties show that these materials are less compressible and elastically stable against deforming force. Pugh's ratio (B/G), Cauchy pressure and Poisson's ratio predicted that these compounds are show brittle behavior. The sound velocities and Debye temperatures are also calculated for these compounds. The higher value of Debye temperatures for DySb compounds reveals that DySb is stiffer than other compounds.

Acknowledgement

We acknowledge the financial support from the Higher Education Commission, Pakistan (HEC), under Start-up Research Grant Program (SRGP), Project no. 1274.

References

1. Pittini R, Schones J, Vogt O, Wachter P (1996) Discovery of 90 degree Magneto-optical Polar Kerr Rotation in CaSb. Phys Rev Lett 77: 944-947.
2. Pittini R, Schones J, Wachter P (1997) Giant magneto-optical Kerr rotation observed in CeS single crystals. Phys Rev B 55:7524-7532.
3. De M, De SK (1999) Electronic structure and optical properties of neodymium mononictides. J Phys Chem Solids 60: 337-346.
4. Sane A, Szotek Z, Temmerman WM, Lægsgaard J, Winter H (1998) J Electronic structure of cerium mononictides under pressure. J Phys Condens Matter 10: 5309-5325.
5. Yakovkin IN, Komesu T, Dowben PA (2002) Band structure of strained Gd(0001) films. Phys Rev B 66: 035406.
6. Gupta DC, Bhat IH (2013) Electronic, ductile, phase transition and mechanical properties of Lu-mononictides under high pressures. J Mol Model 19: 5343-5354.
7. Bhardwaj P, Singh S (2011) High pressure phase transition and elastic properties of covalent heavy rare-earth Antimonides. J Mol Model 17: 3057-3062.
8. Pagare G, Srivastava V, Sanyal SP (2005) Pressure induced

- phase transition in rare earth mono-antimonides. *J Phys Chem Solids* 66: 1177-1182.
9. Leger JM, Ravot D, Mignod JR (1984) Volume behaviour of CeSb and LaSb up to 25 GPa. *J Phys C: Solid State Phys* 17: 4935-4943.
 10. Adachi T, Shirotani I, Hayashi J, Shimomura O (1998) Phase transitions of lanthanide monophosphides with NaCl-type structure at high pressures. *Phys Lett A* 250:389-393.
 11. Shirotani I, Hayashi J, Yamanashi K, Ishimatsu N, Shimomura O, et al. (2001) Pressure-induced phase transitions in lanthanide monoantimonides with a NaCl-type structure. *Phys Rev B* 64: 132101.
 12. Mullen ME, Lüthi B, Wang PS, Bucher E, Longinotti LD, et al. (1974) Magnetic-ion-lattice interaction: Rare-earth antimonides. *Phys Rev B* 10: 186-199.
 13. Rakshit B, Srivastava V, Sanyal SP, Dilawar N, Varandani D, et al. (2008) Lattice vibrational properties of some rare-earth antimonides: Raman scattering measurements and model theory. *Optoelectron Adv Mat* 2: 37-41.
 14. McWhan DB, Vettier C, Longinotti LD, Shirane G (1978) Lattice dynamics of LaSb and PrSb. *Phys Rev B* 18:4540.
 15. Pagare G, Soni P, Srivastava V, Sanyal SP (2009) High-pressure behaviour and elastic properties of heavy rare-earth Gd monopnictides. *J Phys Chem Solid* 70: 650-654.
 16. Gigineishvili AV, Glurjidge LN, Jabua ZU (2011) Optical properties of SmSb and TmSb. *Nano Studies* 3: 19-24.
 17. Missell FP, Guertel RP, Foner S (1997) Magnetic properties of NdSb, GdSb, TbSb, DySb, HoSb and ErSb under hydrostatic pressure. *Solid State Commun* 23: 369-372.
 18. Bhajanker S, Srivastava V, Pagare G, Sanyal SP (2012) Mechanical and thermal properties of praseodymium monochalcogenides and monopnictides under pressure. *J Phys Conf Ser* 377: 012080.
 19. Çoban C, Çolakoglu K, Deligöz E, Çiftçi YÖ (2010) The structural, electronic, elastic, phonon, and thermodynamical properties of the Sm_x (X = P, Sb, Bi) compounds. *Comput Mater Sci* 47:758-768.
 20. Çoban C, Çolakoglu K, Deligöz E, Çiftçi Ö (2011) The first principles study on the TmSb. *Compound Solid State Sci* 13: 1291-1298.
 21. Korozlu N, Colakoglu K, Deligoz E, Surucu G (2010) First-principles study of structural, elastic, lattice dynamical and thermodynamical properties of Gd_x (X= Bi, Sb). *Philos Mag* 90: 1833-1852.
 22. Sane A, Kanchana V, Vaitheeswaran G, Santi G, Temmerman WM, et al. (2005) Electronic structure of samarium monopnictides and monochalcogenide. *Phys Rev B* 71: 045119.
 23. Soni P, Pagare G, Sanyal SP (2010) A theoretical study of structural, elastic and thermal properties of heavy lanthanide monoantimonides. *J Phys Chem Solids* 71: 1491-1498.
 24. Pagare G, Sen D, Srivastava V, Sanyal SP (2010) Study of electronic and structural properties of half metallic rare earth mononitrides. *J Phys Conf Ser* 215: 012114.
 25. Andersen OK (1975) Linear methods in band theory. *Phys Rev B* 12: 3060-3083.
 26. Blaha P, Schwarz K, Madsen GKH, Kuasnicka D, Luitz J (2001) WIEN2k, An Augmented Plane Wave + Local Orbitals Program for Calculating Crystal Properties, K. Schwarz Technical Universitat, Wien, Austria, ISBN 3-9501031-1-2.
 27. Perdew JP, Ruzsinszky A, Csonka GJ, Vydrov OA, Scuseria GE, et al. (2008) Restoring the Density-Gradient Expansion for Exchange in Solids and Surfaces. *Phys Rev Lett* 100:136406.
 28. Jamal M, Asadabadi SJ, Ahmad I, Aliabad HAR (2014) Elastic constants of cubic crystals *Comput Mater Sci* 95: 592-599.
 29. Shafiq M, Arif S, Ahmad I, Asadabadi SJ, Maqbool M, Aliabad HAR (2015) Elastic and mechanical properties of lanthanide monoxides. *J Alloys Compd* 618: 292-298.
 30. Birch F (1947) Finite Elastic Strain of Cubic Crystals. *Phys Rev* 71:809-824.
 31. Duan CG, Sabirianov RF, Mei WN, Dowben PA, Jaswal SS, et al. (2007) Electronic, magnetic and transport properties of rare-earth monopnictides. *J. Phys: Condens Matter*, 19: 315220.
 32. Frantsevich IN, Voronov FF, Bokuta SA (1983) Elastic Constants and Elastic Moduli of Metals and Insulators, Handbook, ed. by Frantsevich IN, Naukova Dumka, Kiev, 60-180.
 33. Vaitheeswaran G, Kanchana V, Rajagopalan M (2002) Electronic and structural properties of LaSb and LaBi. *Physica B* 315: 64-73.
 34. Shoaib M, Murtaza G, Khenata R, Farooq M, Ali R (2013) Structural, elastic, electronic and chemical bonding properties of AB (A = Sc, Y, La; B = N, P, As, Sb, Bi) from first principles. *Comput Mater Sci* 79: 239-246.
 35. Vaitheeswaran G, Petit L, Sane A, Kanchana V, Rajagopalan M (2004) Electronic structure of praseodymium monopnictides and monochalcogenides under pressure. *J. Phys: Condens Matter* 16: 4429-4440.
 36. Soni P, Pagare G, Shrivastava V, Sanyal SP (2009) Study of high pressure behavior and elastic properties of praseodymium monochalcogenides and monopnictides. *Phase Transition* 82:519-530.
 37. Hayashi J, Shirotani I, Tanaka Y, Adachi T, Shimomura O, et al. (2000) Phase transitions of LnSb (Ln=lanthanide) with NaCl-type structure at high pressures. *Solid State Commun* 114: 561-565.
 38. Shirotani I, Yamanashi K, Hayashi J, Ishimatsu N, Shimomura O, et al. (2003) Phase transitions of LnSb (Ln=lanthanide) with NaCl-type structure at high pressures. *Solid State Commun* 127: 573-576.
 39. Bokhara N, Abidri B, Hiadsi S, Rached D, Rabah M, et al. (2011) Study of structural, elastic and electronic properties of Gd_x (X= Bi, Sb) compounds using LSDA and LSDA+U approach. *Comput Mater Sci* 50: 1965-1972.
 40. Mitra C, Lambrecht WRL (2008) Magnetic exchange interactions in the gadolinium pnictides from first principles. *Phys Rev B* 78:134421.
 41. Sahu AK, Singh A, Prafulla KJ, Sanyal SP (2011) Pressure-induced structural phase transition and electronic properties of RESb (RE = Ho, Er and Tm) compounds: ab initio calculations. *Phase Transitions* 84: 603-612.
 42. Gupta DC, Singh SK (2012) Structural phase transition, elastic and electronic properties of TmSb and YbSb: A LSDA + U study under pressure. *J Alloys Compd* 515: 26-31.
 43. Abdusalyamova MN, Rakhmatov OI (2002) Thermal Expansion of TmSb, TmTe, and Their Solid Solutions TmSb_{1-x}TmTe_x. *High Temperature* 40:636-637.
 44. Hulliger F, in: Gschneidner KAEyring L (1979) (Eds.), Handbook on the Physics and Chemistry of Rare Earths, North-Holland, Amsterdam 4: 153.
 45. Hayashi J, Shirotani I, Adachi T, Shimomura O, Kikegawa T (2004) Phase transitions of Yb_x (X=P, As and Sb) with a NaCl-type structure at high pressures. *Philos. Mag.*, 84:3663-3670.
 46. Singh D, Pandey DK, Singh DK, Yadav RR (2011) Propagation of ultrasonic waves in neptunium monochalcogenides. *Applied Acoustics* 72: 737-741.

47. Kaurav N, Kuo YK, Joshi G, Choudhary KK, Varshney D (2008) High-pressure structural phase transition and elastic properties of yttrium pnictides. *High Pressure Research* 28: 651-663.
48. Wallace DC (1972) *Thermodynamics of Crystals*. John Wiley Sons, New York.
49. Born M, Huang K (1954) *Dynamical Theory of Crystal Lattices*. Clarendon, Oxford.
50. Varshney D, Shriya S, Varshney M (2012) Study of pressure induced structural phase transition and elastic properties of lanthanum pnictides. *Eur Phys J B* 85: 241.
51. Tutuncu HM, Bagci S, Srivastava GP (2007) Electronic, elastic and phonon properties of the rock-salt LaSb and YSb. *J Phys Condens Matter* 19: 156207.
52. Yadav R, Singh D (2001) Behaviour of ultrasonic attenuation in intermetallics. *Intermetallics*, 9: 189-194.
53. Hill R (1952) The Elastic Behaviour of a Crystalline Aggregate. *Proc Phys Soc Lond A* 65: 349-354.
54. Voigt W (1889) Uber die Beziehung zwischen den beiden Elasticitätsconstanten isotroper Körper. *Ann Phys* 38: 573-587.
55. Reuss A, *Angew Z* (1929) Berechnung der Fließgrenze von Mischkristallen auf Grund der Plastizitätsbedingung für Einkristalle. *Math Phys* 9: 49-58.
56. Pugh SF (1954) XCII. Relations between the elastic moduli and the plastic properties of polycrystalline pure metals. *Philos Mag* 45: 823-843.
57. Pettifor DG (1992) Theoretical predictions of structure and related properties of intermetallics. *Mater Sci Technol* 8: 345-349.
58. Greaves GN, Greer AL, Lakes RS, Rouxel T (2011) Poisson's ratio and modern materials. *Nat Mater* 10: 823-837.
59. Kim K, Lambrecht WRL, Segal B (1994) Electronic structure of GaN with strain and phonon distortions. *Phys Rev B* 50: 1502-1505.
60. Kleinman L (1962) Deformation Potentials in Silicon. I. Uniaxial Strain. *Phys Rev* 128: 2614-2621.
61. Harrison WA (1989) *Electronic Structure and Properties of Solids*. Dover New York.
62. Mayer B, Anton H, Bott E, Methfessel M, Sticht J, et al. (2003) Ab-initio calculation of the elastic constants and thermal expansion coefficients of Laves phases. *Intermetallics* 11: 23-32.
63. Johnston I, Keeler G, Rollins R, Spicklemire S (1996) *Solid State Physics Simulations, The Consortium for Upper-Level Physics Software*. Wiley, New York.
64. Shafiq M, Ahmad I, Asadabadi SJ (2014) Theoretical studies of strongly correlated rare-earth intermetallics RIn₃ and RSn₃ (R=Sm, Eu, and Gd). *J Appl Phys* 116: 103905.
65. Anderson OL (1963) A simplified method for calculating the Debye temperature from elastic constants. *J. Phys. Chem. Solids* 24: 909-917.
66. Schreiber E, Anderson OL, Soga N (1973) *Elastic Constants and Their Measurements*. McGraw-Hill New York.

Copyright: ©2018 Muhammad Shafiq, et al. This is an open-access article distributed under the terms of the Creative Commons Attribution License, which permits unrestricted use, distribution, and reproduction in any medium, provided the original author and source are credited.